

# COUPLER DESIGN FOR THE LCLS INJECTOR S-BAND STRUCTURES\*

Zenghai Li, Jose Chan, Lynn D. Bentson, David H. Dowell,  
Cecile Limborg-Deprey, John F. Schmerge, David Schultz, Liling Xiao, SLAC, USA

## Abstract

The LCLS injector is required to provide a 1-nC, 10-ps bunch with a normalized rms transverse projected emittance of less than 1 micron. The LCLS beam is generated and accelerated in a 1.6-cell S-band RF gun at 120 MV/m up to 6 MeV. The gun is followed by two SLAC 3-m S-band accelerator structures to further accelerate the beam to 135 MeV which moves the beam out of the space-charge dominated regime. In the SLAC S-band structures, the RF power feed is through a single coupling-hole (single-feed coupler) which results in a field asymmetry. The time dependent multipole fields in the coupler induce a transverse kick along the bunch and cause the emittance to increase above the LCLS specification. To meet the stringent emittance requirements for the injector, the single-feed couplers will be replaced by a dual-feed racetrack design to minimize the multipole field effects. We will present detailed studies of the multipole fields in the SLAC linac RF coupler and the improvements with the dual-feed racetrack design using the parallel finite element S-parameter solver S3P.

## INTRODUCTION

The electron beam in the LCLS[1] injector is produced and accelerated to 6 MeV in a 1.6-cell S-band photo RF gun[2]. Two SLAC 3-m S-band accelerator structures operating at 19.5 and 25 MV/m gradient, are used to accelerate the beam out of the space charge dominated regime. In the SLAC S-band structure, the RF power feed is through a single coupling hole. Time dependent multipole fields in the coupler induce transverse kicks along the bunch, causing head-tail beam emittance degradation, which is important for the LCLS injector beams because of the stringent emittance requirement. In the results presented in ref[3], the measured asymmetries in the SLAC structure coupler take the form of a linear amplitude and phase variation across the coupler cell as expressed in Eq.[1].

$$E_z = E_{z0} \left[ 1 + \frac{\Delta E}{E_{z0}} \frac{x}{2a} \right] e^{j(\alpha x - k_z + \Delta\Phi \frac{x}{2a})} \quad (1)$$

where  $\Delta E/E$  is approximately 0.001 (was 0.1 before compensating by offsetting the coupler cell center) and  $\Delta\Phi$  is approximately  $1.5^\circ$ . The transverse variation of  $E_z$  field creates a transverse magnetic field which deflects the beam. The estimated head-tail deflection angle for a 10-ps bunch is about 200 micro-radian in the first injector linac coupler, which is dominated by the phase related dipole term. The quadratic field terms for the SLAC coupler were not reported so the quadrupole effects cannot be

estimated. The head-tail effect results in a projected emittance increase which can be estimated using Eq. 2.

$$\epsilon_{n-final} = \sqrt{\epsilon_{n-initial}^2 + \sigma_x^2 \left( \frac{\sigma_{\Delta p_x}}{mc} \right)^2} \quad (2)$$

For a dipole head-tail angle of 200 micro-radian, the estimated RMS emittance increase is about 2%/12% with an initial emittance of 1 micron and beam size of 1 mm for the first and second linac sections respectively[5]. This 2%/12% emittance increase is not acceptable for the LCLS beam so the dipole fields in the coupler must be reduced. Compensating the head-tail kicks using transverse wakefield would not be a satisfying solution for all possible beam parameters. Since the dipole term is mainly due to the phase asymmetry, a viable solution to reduce the dipole head-tail effect is to replace the single-feed coupler with a dual-feed design. In addition, a racetrack cell profile will be needed to minimize the quadrupole fields. In this paper, we will present the design and analysis of the new dual-feed racetrack coupler for the LCLS injector S-band structures.

## TOLERANCE ON MULTIPOLE FIELDS

As seen in equation 2, the normalized emittance increase is independent of energy, but depends on the square of the beam size and thus is typically most important in the injector where the beam size is large. Numerical studies on the tolerances on dipole and quadrupole head-tail effects in the coupler cell of the LCLS injector linacs have been performed using PARMELA. In the PARMELA simulations, the head-tail kicks were introduced at the entrance of the coupler cell as a single kick. The dipole kick was represented by a linear angle offset from head-to-tail and the quadrupole kick was introduced as a linear quadrupole strength varying from head-to-tail. For both cases, we looked at the growth of the 80%-emittance (over 100 slices). Transverse wakefield effects were included. The emittance degradation a function of the dipole and quadrupole head-tail angles is shown in Fig 1.

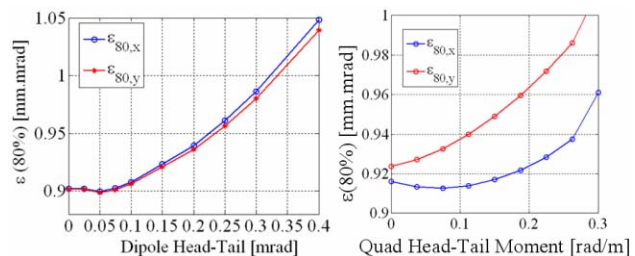


Figure 1: PARMELA results of emittance degradation due to dipole and quad head-tail effects in the linac couplers.

\* Work supported by the U.S. DOE Contract No. DE-AC02-76SF00515.

The tolerance on the kick is set by limiting the emittance growth to 2%. For the dipole kick, the angle difference should not be larger than 120 micro-radian from head-to-tail of a 10-ps bunch as illustrated in Fig. 1. For the quadrupole kick, the quadrupole moment should not exceed 0.1 rad/m from head-to-tail of a 10 ps bunch. Allowing the possibility to operate with 20 ps long pulses, the actual tolerances are 60 micro-radian for the dipole and 0.05 rad/m for the quadrupole. Based on the analytical estimations, the dipole deflection in the coupler must be reduced by at least a factor of 4 below the existing value in order to reduce the emittance growth to acceptable levels.

## MULTIPOLE ANALYSIS

The parallel finite element S-parameter code S3P[4] is used to calculate the coupler matching and the full 3-D RF fields in the coupler. The impact of the coupler fields on the beam dynamics is studied by analyzing the particle momentum change after traversing the coupler fields. The equation of motion

$$\frac{d(\gamma\vec{\beta})}{dt} = \frac{e}{m_0c} (\vec{E} + c\vec{\beta} \times \vec{B}) \quad (3)$$

is integrated through the coupler field. The transverse momentum change,  $\Delta(\gamma\vec{\beta})$ , is Fourier decomposed into multipole terms according to the following equation

$$\Delta(\gamma\vec{\beta}_\perp) = A_0(x\vec{x}_0 + y\vec{y}_0) + D_x\vec{x}_0 + D_y\vec{y}_0 + Q(y\vec{y}_0 - x\vec{x}_0) + S(y\vec{x}_0 + x\vec{y}_0) \quad (4)$$

where  $A_0$  is the RF focusing,  $D_x/D_y$ ,  $Q$  and  $S$  are the dipole, quadrupole and skew quadrupole components respectively.

## SINGLE-FEED SLAC STRUCTURE

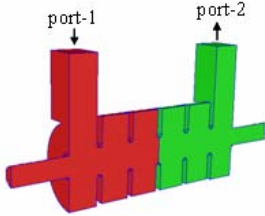


Figure 2: Symmetric single-feed coupler model used in S3P simulation.

In the S3P simulations, a two-port network is required to calculate the S-parameters and the traveling wave fields. Back-to-back symmetric models as shown in Fig. 2 were built for the input and output couplers respectively. The 3D traveling RF fields in the coupler models were obtained by driving “port-1” with a TE10 mode. In the beam dynamics studies only the field in the “port-1” side is used for the input coupler and only the field in the “port-2” side is used for the output coupler. The transverse dipole and quadrupole moments of the coupler fields, at a gradient of 20 MV/m, as functions of beam RF phase, where zero phase is the RF crest, are plotted in Fig. 3. The thick line segments indicate the RF

phase of a 10 degree long bunch. Table 1 lists the head-tail momentum ( $\Delta(\gamma\beta_\perp)$ ) and steering angle ( $\Delta(\gamma\beta_\perp)/\gamma$ ) for a bunch accelerated -10 degrees off crest.

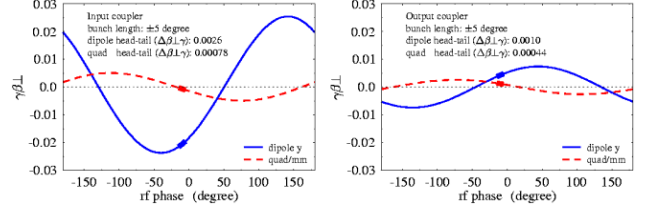


Figure 3: Head-tail effect of SLAC 3-m structure: left) dipole field; right) quadrupole field. The thicker line segment represents the 10 degree bunch.

Table 1: Dipole and quadrupole head-tail effects in the SLAC 3-m structure input/output couplers.

	Input	Output
Beam energy ( $\gamma$ )	10	130
Dipole: $\Delta(\gamma\beta_\perp)$	$2.6 \times 10^{-3}$	$1.0 \times 10^{-3}$
Quad: $\Delta(\gamma\beta_\perp)/m$	$7.8 \times 10^{-1}$	$4.4 \times 10^{-1}$
Dipole head-tail angle (rad)	$2.6 \times 10^{-4}$	$7.7 \times 10^{-6}$
Quad head-tail angle (rad/m)	$7.8 \times 10^{-2}$	$3.4 \times 10^{-3}$

Numerical results have shown that both the dipole and quadrupole head-tail effects in the input couplers of both injector linacs are larger than the tolerance set by the emittance criteria. In the output coupler, the head-tail effects are about 4 times smaller than in the input coupler and found to be acceptable. Thus only the input couplers need to be replaced by a more symmetric design.

## DUAL-FEED INPUT COUPLER

The dual-feed scheme includes a power distribution waveguide system and a dual-feed coupler, as shown in Fig. 4. The design approach of such a system is to use as much standard parts as possible to save cost. With this in mind, the coupler port dimension in the new design is increased to the full dimension of the WR284 waveguide. The tapers are eliminated and standard WR284 flanges can be used. The power splitter is a simple WR284 “T” and the 180 degree waveguide bend can be made by bending the standard WR284 waveguide.

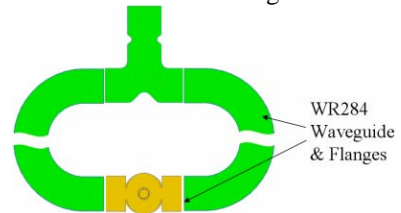


Figure 4: Dual-feed waveguide system. The coupler port dimensions are the same as the WR284 waveguide to simplify the system.

### Dual-feed coupler optimization

The dual-feed coupler eliminates both geometric and phase related dipole fields by symmetry. The design focuses upon matching the coupler and minimizing the quadrupole term using a racetrack cell. A sketch of the

dual-feed racetrack coupler is shown in Fig. 5. The left figure shows the racetrack profile of the coupler cell. The two (+) symbols indicate the centers of two racetrack arcs. The separation of the two arc centers is optimized to reduce the quadrupole field. The edges of the coupling irises are rounded to minimize possible field enhancement and RF heating. The left figure shows the coupler cell with the length of the full WR284 height, which is about 5-mm longer than a regular  $2\pi/3$  cell. The design was done iteratively by adjusting the arc separation to minimize quadrupole fields and adjusting the iris opening and the arc radius to match the coupling. After a number of iterations, a factor of 10 reduction in quadrupole field and a less than 0.02 reflection were achieved. The phase dependent quadrupole field in the present dual-feed racetrack design is shown in Fig 6 to compare with the original single-feed design and the dual-feed design with the cylindrical cell. The head-tail kick angles for a 10 degree bunch are shown in Table 2. The dual feed with racetrack design is approximately 20 times smaller than the single feed case because the peak quadrupole term is smaller and the curve is flat at the desired operating phase. The design is about an order of magnitude better than the tolerance level.

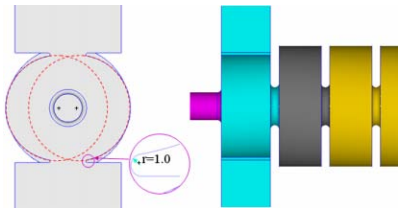


Figure 5: Dual-feed coupler with racetrack cell profile to minimize dipole and quadrupole fields.

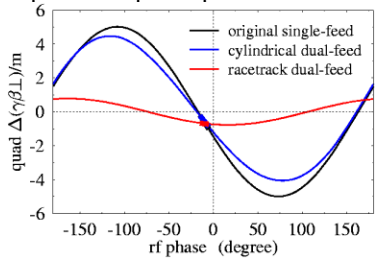


Figure 6 Quadrupole moments in the dual-feed racetrack coupler. The quadrupole moments in the single-feed and the cylindrical dual-feed are shown for comparison.

Table 2: Comparison of quadrupole kick angles

Input coupler: comparison of quad head-tail $\Delta(\gamma\beta_{\perp})/m$ : 10 Degree bunch		
	$\Delta(\gamma\beta_{\perp})/m$	HT angle $\Delta\theta$ (rad/m)
Single feed	0.78	0.078
Symmetric dual	0.63	0.063
<b>Race-track dual</b>	<b>0.04</b>	<b>0.004</b>

#### Dimension Tolerance on Field Asymmetry

Machine/construction errors and RF feed imbalance of the dual-feed coupler will result in field asymmetry in the coupler cell. We consider the effects of four errors: a) Coupler position (not 180 degrees apart); b) Coupler iris

size; c) RF feed amplitude; and d) RF feed phase. As an analogy to Eq.1, the fields in a dual-feed coupler cell can be expressed as the following:

$$E_z = \frac{E_{z0}}{N} \sum_{i=1}^2 \frac{V_i D_i}{V_0 D_0} \left[ 1 + \frac{\Delta E}{E_{z0}} \left( \sin \theta_i \frac{x}{2a} + \cos \theta_i \frac{y}{2a} \right) \right] e^{j \left[ \Phi_0 + \frac{D_i}{D_0} \Delta \Phi \left( \sin \theta_i \frac{x}{2a} + \cos \theta_i \frac{y}{2a} \right) \right]} \quad (5)$$

where  $V_0$  is the amplitude necessary to produce an accelerating gradient  $E_{z0}$  and  $D_0$  is the nominal dimension of the coupler iris.  $V_i$ ,  $D_i$  and  $\theta_i$  are the complex amplitude, coupling iris dimension and coupling iris angular position of the  $i^{\text{th}}$  coupler respectively. The criteria used for acceptable tolerance were that the dual feed dipole term in Eq. 5 must be reduced by a factor of 100 from a single feed structure, and the quadrupole term must be reduced by a factor of 10. Table 3 lists the error and the corresponding tolerance as well as the criteria setting the tolerance for the four errors described above.

Table 3: The tolerance for the four coupler errors.

Error	Tolerance	Defining Criteria
Coupler Position	$\Delta\theta < 1.1^\circ$	Dipole
Coupler Iris Size	$\Delta D/D_0 < .02$	Dipole
RF Feed Amplitude	$\Delta V/V_0 < .02$	Dipole
RF Feed Phase	$\Delta\alpha < 1.1^\circ$	Dipole

All errors were considered independently. Thus multiple simultaneous errors will produce larger dipole and quadrupole terms than desired. However, the coupler position tolerance is quite loose. The coupler iris size is also relatively loose. The RF amplitude tolerance will be challenging but in principle can be reached by tuning the RF power splitter. The RF phase error can in principle be set to  $1^\circ$  by measurement and waveguide phase tuning so phase errors do not appear to be problematic.

## SUMMARY

The multipole fields in the single-feed SLAC S-band structure are analyzed and found to be larger than the acceptable level for the LCLS injector accelerator sections. A dual-feed racetrack coupler has been designed to replace the single-feed input coupler. The new design eliminated the dipole fields by symmetry and reduced the quadrupole field by a factor of 10. The tolerance on the dual-feed geometry and RF errors were analyzed and found to be achievable. The mechanical design for the new coupler is in progress.

## REFERENCE

- [1] <http://www-ssrl.slac.stanford.edu/lcls>
- [2] Liling Xiao, et al, "Dual-feed RF Gun Design for LCLS," this proceedings.
- [3] The Stanford Two-Mile Accelerator, Edited by R.B. Neal, 1968, W.A. Benjamin Inc, pg 146.
- [4] L. Lee, et al., "Solving Large Sparse Linear Systems in End-to-end Accelerator Structure Simulations," Proceedings of the 18th International Parallel and Distributed Processing Symposium, 2004.
- [5] C.Limborg-Deprey et al. "RF Modifications in the LCLS Injector Beamline," this proceedings.